

Coevolutionary search for optimal materials in the space of all possible compounds

Zahed Allahyari^{1,2} and Artem R. Oganov^{1,2,3}

¹*Skolkovo Institute of Science and Technology, Skolkovo Innovation Center, 3 Nobel St., Moscow 143026, Russia*

²*Moscow Institute of Physics and Technology, 9 Institutskiy Lane, Dolgoprudny city, Moscow Region, 141700, Russian*

³*International Center for Materials Design, Northwestern Polytechnical University, Xi'an, 710072, China*

December 14, 2024

Over the past decade, evolutionary algorithms, data mining and other methods showed great success in solving the main problem of theoretical crystallography: finding the stable structure for a given chemical composition. Here we develop a method that addresses the central problem of computational materials science: prediction of material(s), among all possible combinations of all elements, that possess the best combination of target properties. This non-empirical method combines our coevolutionary approach with carefully restructured "Mendeleevian" chemical space, energy filtering, and Pareto optimization to ensure that the predicted materials have optimal properties and a high chance to be synthesizable. First calculations, presented here, illustrate the power of this approach.

Keyword: Coevolutionary algorithm; evolutionary algorithm; hardness; Mendeleev numbers; multi-objective optimization

1. Introduction

Discovery of materials with optimal properties (e.g., highest hardness, lowest dielectric permittivity, etc) or combination of properties (e.g., highest hardness and fracture toughness) is the central problem of material science. Until recently, only experimental materials discovery was possible with all limitations and expense of trial-and-error approach, but due to the ongoing revolution in theoretical/computational materials science, the situation begins to change. Using quantum-mechanical calculations, it is now routine to predict many properties when the crystal structure is known. In 2003, Curtarolo demonstrated data mining method for materials discovery¹ by making use of crystal structure databases (which can include known or hypothetical structures) and screening them with *ab initio* calculations. At the same time, major progress in fully non-empirical crystal structure prediction took place. Metadynamics² and evolutionary algorithms³⁻⁵ have convinced the community that crystal structures are predictable. Despite success of these and other methods, a major problem remains unsolved – that of predicting, among all possible compounds, a material with optimal properties. With 118 known elements in the Periodic Table, only by considering a hundred best-studied elements, 4950 binary systems, 161700 ternary systems, 3921225 quaternary systems and an exponentially growing number of systems of increasing complexity can be created. In each system, a very large number of compounds and, technically, infinity of crystal structures can be constructed computationally – and direct screening of such a multitude is impractical. Ex-

perimentally, only about 72% of binary, 16% of ternary, 0.6% of quaternary and less than 0.05% of more complex systems have ever been studied⁶ and even in those systems that have been studied, new compounds are continually discovered⁷⁻⁹. Studying all these systems, one by one, using global optimization methods is unrealistic. Data mining is a more realistic approach, but the above statistics show that existing databases are significantly incomplete even for binary systems, while for ternary and more complex systems data mining would be problematic. Besides, data mining cannot come up with fundamentally new crystal structures. When searching for materials optimal in more than one property, these limitations of both approaches become even greater. We present a new method that we implemented in our code, MendS (Mendeleevian Search), and show its application to discovery of (super) hard and magnetic materials.

2. Mendeleevian Space

Global optimization methods are effective only when applied to property landscapes that have an overall organization - e.g. landscape with a small number of funnels. In order to discover materials with optimal properties, i.e. solve a complex global optimization in chemical and structural space, we must rationally design the chemical space, so that compounds with similar properties are nearby in this chemical space. If this space is created by ordering the elements by their atomic numbers, instead of having similar systems clustered together, we will observe a periodic patchy pattern (Fig 1a). In 1984, Pettifor suggested a new quantity, the so-called "chemical scale" that arranges elements in a sequence, such that similar elements are placed near each other, and compounds of these elements also display similar properties¹⁰. This way, structure maps¹¹, with well-defined

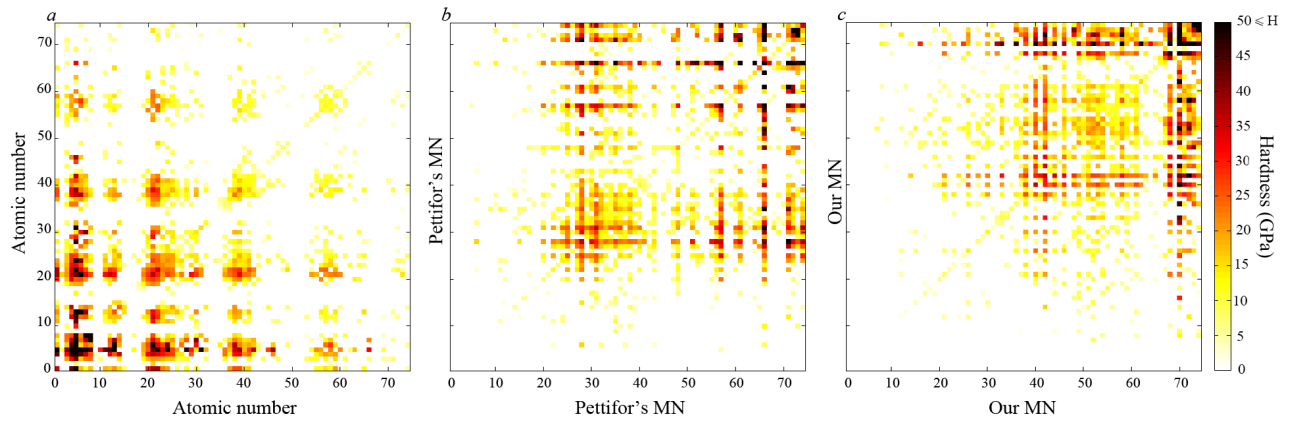


Figure 1: Pettifor maps showing hardest materials for all binary systems, using: *a*) Atomic numbers, *b*) Pettifors MN *c*) MN obtained in our work. Noble gases, rare earths, and elements heavier than Pu were excluded: noble gases due to their almost complete inability to form stable compounds at normal conditions, and rare earth and actinide elements due to problems of DFT calculations. In total, we consider 74 elements, which can be combined into 2775 possible binary systems.

regions of similar crystal structures or properties, can be drawn. In the thus ordered chemical space, evolutionary algorithms should be extremely effective.

What is the nature of the chemical scale (or the Mendeleev number, which is an integer showing of the sequence of elements on the chemical scale)? Pettifor derived these quantities empirically, while we redefined them¹² using a non-empirical (thus, more universal) way, which clarifies their physical meaning. In redefining these quantities, we used the most important chemical properties of an atom (size R and electronegativity χ) in which the combination of these properties can be used as a single parameter succinctly characterizing chemistry of the element. However, we need to emphasize that these quantities (chemical scale and MN) are only used for visualizing the results, while within our global coevolutionary algorithm, each atom is represented by both properties (size R and electronegativity χ). Fig 2a shows the overall linear correlation between Pettifor's and our Mendeleev numbers. Good Mendeleev numbers will lead to strong clustering in the chemical space, where neighboring systems have similar properties. This gives a means to evaluate our new Mendeleev number. Fig 1-b,c shows the Pettifor map constructed on the results of our searches for hard binary compounds using the MN suggested by Pettifor, and our redefined MN. Satisfyingly, our redefined MN gives even better-organized chemical space with clearer separation of regions containing binary systems with similar hardness. In this paper, we illustrate our method on binary systems, although more complex systems (at least ternary) are tractable.

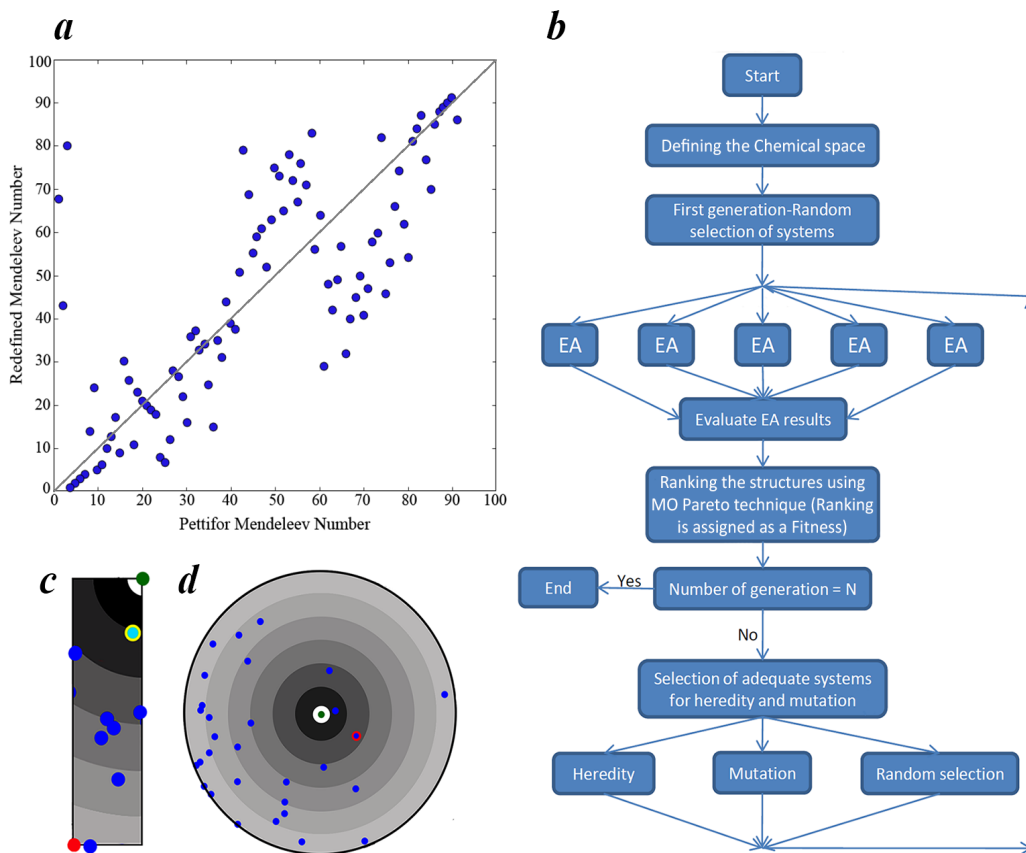


Figure 2: a) Relationship between our and Pettifor's Mendeleev numbers b) The coevolutionary algorithm used in MendS. Schematic figure showing how chemical heredity (c) and chemical mutation (d) create new compositions. In these figures, the probability (demonstrated by dark to light circles) is given to each possible child according to his distance from the fitter parent (green point).

3. Method

The whole process can be described as a joint evolution (or coevolution) of evolutionary runs (each of which deals with an individual binary variable-composition system). Having defined the chemical space, we initialize the calculation by randomly selecting a small number of systems from the entire chemical space for the first MendS generation. These systems are then optimized by the evolutionary algorithm USPEX³⁻⁵ in its variable-composition mode¹³, searching for compounds and structures with optimal properties (in our example, we simultaneously maximized hardness and stability), after which MendS jointly analyses results from all these systems. Removing identical structures using fingerprint method¹⁴, jointly evaluating all systems, refining and preparing the dataset and discarding structures which are unstable by more than 1.0 eV/atom, MendS ranks all the systems of the current generation and selects (usually 70%) fittest systems as potential parents for new systems. Applying variation operators (such as mutation and heredity) to these parent systems, offspring systems for the next coevolutionary generation are obtained. Additionally, some systems are generated randomly to preserve chemical diversity of the population. This process is continued until the number of coevolutionary generations reaches the maximum predefined by the user (Fig 2b).

3.1. Defining fitness: Multi-Objective (Pareto) optimization

Many scientific and engineering problems involve optimization of multiple conflicting objectives; for example, the goal of a materials scientist is to predict novel materials that improve upon all

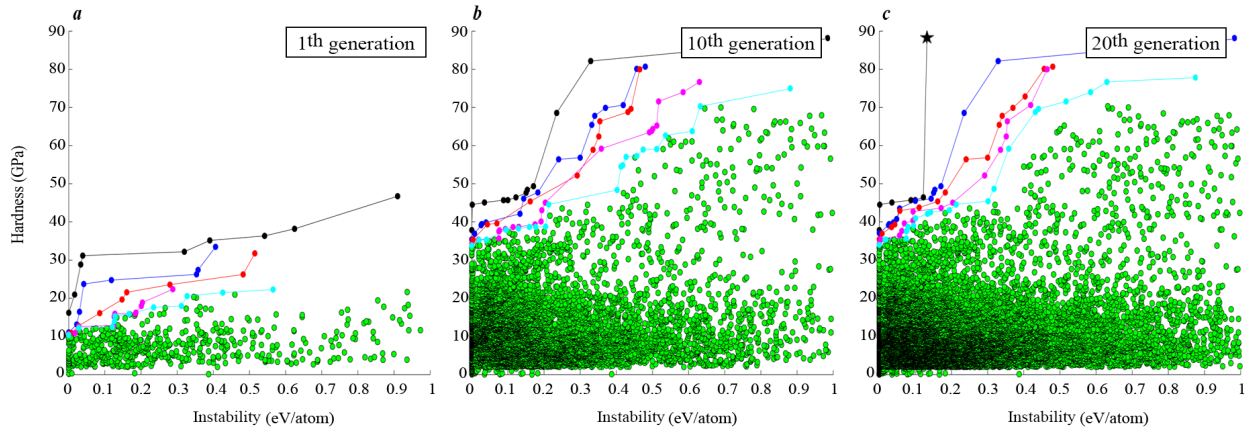


Figure 3: Results of simultaneous optimization of hardness and stability in the space of all binary and unary compounds: *a*) 1st MendS generation, *b*) 10th MendS generation, *c*) 20th MendS generation. First five Pareto fronts are shown, green points represent all sampled structures. Instability of each compound is defined using Maxwell’s convex hull construction. Star shows diamond - the hardest material.

critical properties of the known materials. To that end, multi-objective evolutionary algorithm (MOEA), enables searching for materials with multiple optimal properties simultaneously, such as enthalpy, hardness, density, dielectric permittivity, magnetization, etc. Here, we performed searches for materials that optimize simultaneously (1)stability (measured as the distance above convex hull) and (2)hardness, computed using Lyakhov-Oganov model¹⁵. The results of multi-objective optimization are, in general, not a single material, but a set of materials with trade-off between their properties, and these optimal materials form the so-called first Pareto front. Similarly, 2^{nd} , 3^{rd} , ... n^{th} Pareto fronts can be defined. In our scheme, Pareto rank is used as fitness.

3.2. Variation operators in the chemical space: these are of central importance for efficient sampling of the chemical space, making use of the previously sampled compositions and structures. These operators ensure that different populations not only compete, but also learn from each other. One can construct an efficient algorithm where the chemical space is defined by just one number for each element - the Mendeleev number (or chemical scale); we use this for plotting Pettifor maps, but within the algorithm itself, each element is described by two numbers - electronegativity χ and radius R , rescaled to be between 0 and 1 - and it is this space where variation operators act. There are three variation operators defined in the chemical space:

Chemical heredity replaces elements in parent systems with new elements such that their electronegativities and atomic radii lie in between the values of their parents (Fig 2c). In doing so, we explore regions of the chemical space between parents.



where X is between A and C or A and D which is chosen randomly, and Y is between the other two elements (B and D or B and C).

Reactive heredity creates offspring by taking combinations of the elements from parents. For example, if the parents are $A-B$ and $C-D$, their child is one of $A-C, A-D, B-C$ and $B-D$ systems.

Chemical mutation randomly chooses one of the elements of the parent, and substitutes it with another element in its vicinity in the space of χ and R (Fig 2d).

In both chemical mutation and chemical heredity, a probability is given to all elements:

$$P_i = \frac{e^{-\alpha x_i}}{\sum e^{-\alpha x_i}}, \quad i = 1, 2, \dots \quad (2)$$

where x is the distance of element i from the parent element (in the case of chemical heredity, we use this formula to give higher weight to the fitter parent – green point in Fig.2c), and α is a constant (here we use $\alpha = 1.5$). Fig.4 illustrates the power of these variation operators in sampling the chemical space: it is clear that promising regions of the chemical space are sampled more thoroughly at the expense of unpromising regions. We note that when a new system is produced from parent system(s), it inherits a set of optimal crystal structures from parent(s) and these are added to the first generation, which greatly enhances the learning power of the method.

When the coevolutionary simulation was finished, we took the most promising systems identified in it, performed longer evolutionary runs for each of them, and calculated final hardness using Chen-Niu model¹⁶ and fracture toughness using Niu-Niu-Oganov model¹⁷. Some of these results were already reported by us in a separate paper on *Cr-B*, *Cr-C*, *Cr-N* systems¹⁸ and our study of the *W-B* system¹⁹ was inspired by present finding of promising properties in the *Mo-B* system. Below, we discuss new results.

4. Results and Discussion

Pareto optimization of the hardness and stability was performed over all possible structures (with up to 12 atoms in the primitive cell) and compositions limited to all possible binary compounds of 74 elements (i.e. all elements excluding noble gases, rare earth elements and elements heavier than Pu). In this calculation, 600 systems have been computed in 20 MendS generations from a total of 2775 binary and unary systems that can be made of 74 elements, i.e. only about one fifth

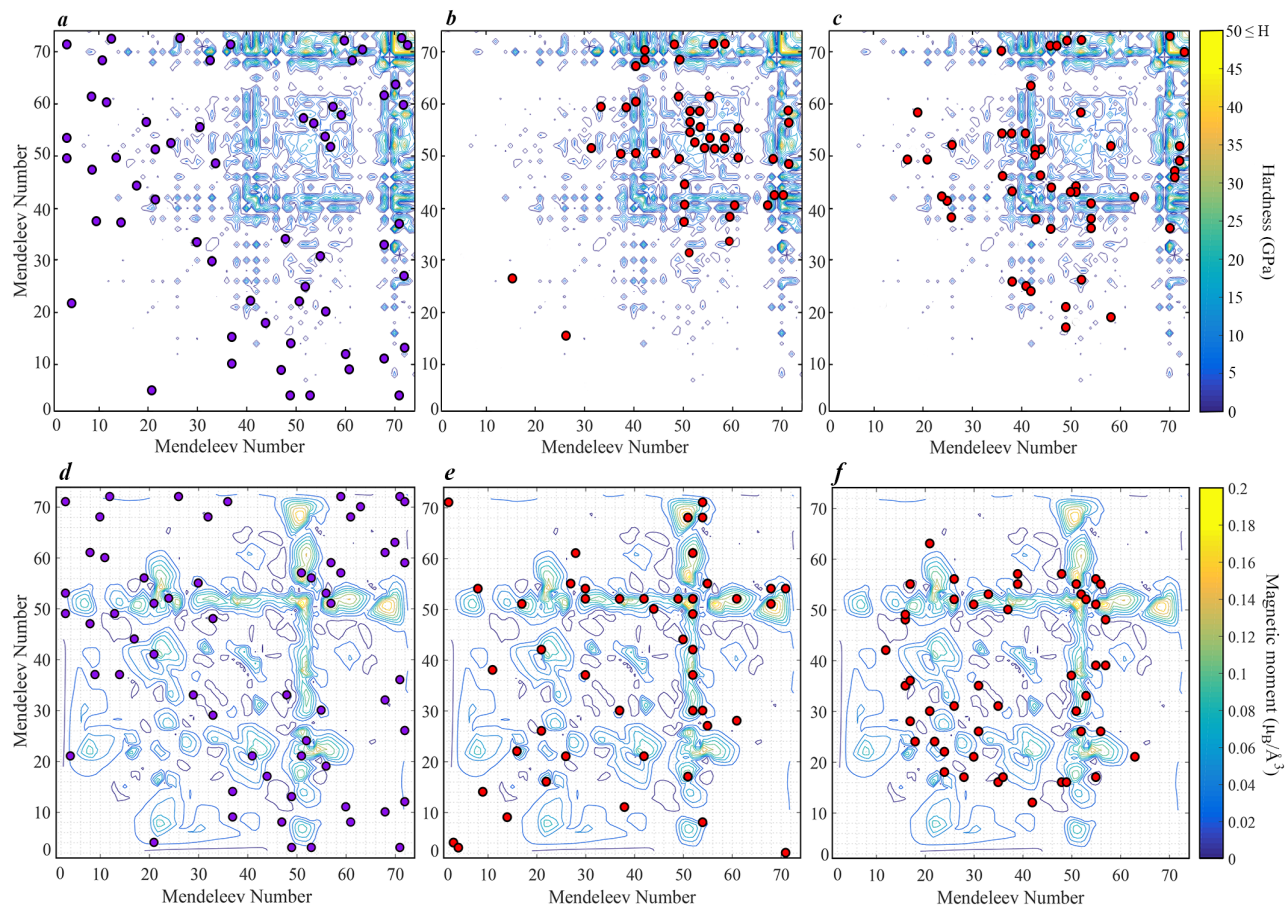


Figure 4: Selected systems *a*) randomly in the 1st, and using all variation operators in the *b*) 5th, and *c*) 10th generations in searching for hard (a-c) and magnetic (d-f) materials. Randomly generated systems are shown with violet circles.

of all the systems were sampled by MendS. Fig.3 shows the efficiency of our method in finding optimal materials. In this fast calculation, numerous stable and metastable hard and superhard materials were detected as a result of this single run. Among the elements, carbon (diamond and other allotropes) and boron, known to be the only superhard elements, were both found. Excitingly, in addition to different allotropes of carbon and boron, both new and numerous already known hard and superhard binary systems as well as the systems, claimed to have a potential to be hard, were found in our calculation. B_xC_y ²⁰⁻²², C_xN_y ^{23,24}, B_xN_y ^{25,26}, B_xO_y ^{20-22,27}, Re_xB_y ^{28,29}, W_xB_y ³⁰, Si_xC_y ³¹⁻³⁵, W_xC_y ³³⁻³⁵, Al_xO_y ³³⁻³⁵, Ti_xC_y ³⁵, Si_xN_y ³⁵, Ti_xN_y ³⁵, Be_xO_y ³⁵, Ru_xO_y ^{36,37}, Os_xO_y ³⁸, Rh_xB_y ³⁹, Ir_xB_y ³⁹, Os_xB_y ⁴⁰⁻⁴² and Ru_xB_y ⁴⁰⁻⁴² can be mentioned as a few sample systems discussed in the literature and found by us in this single calculation. The list of all systems studied during the calculation is available in Supplementary Information. Due to the huge compositional space (2775 systems, each with 10^2 possible compositions, each with an astronomically large number of possible structures), it was necessary to reduce the time of calculations by means of reducing the number of generations and/or population size. With reduced computational settings, structures and compositions may be approximate and may need to be refined by a precise evolutionary calculation on each of these systems. Table 1 shows the results on some of the selected promising systems which were further studied using evolutionary calculation. Of these, some transition metal borides are predicted to be hard, some of them have been reported as hard materials i.e. Mo_xB_y ^{43,44}, Mn_xB_y ⁴⁵ or have been discussed to have a potential to be hard i.e. Tc_xB_y ⁴⁶, Fe_xB_y ⁴⁷ and V_xB_y ⁴⁸. Interestingly, a number of previously unknown hard structures that are more stable than previously reported structures were predicted in these systems (Table 1). More im-

portantly, as shown in Table 1, even completely new hard systems were revealed in our run, i.e. S_xB_y and B_xP_y , and quite an unexpected system i.e. Mn_xH_y is discovered to contain very hard phases. For Mo_xB_y system, several simultaneously hard and low-energy structures were detected in our calculation. Of these, only the stable $R\bar{3}m$ structure of MoB_2 was studied before and the reported hardness (24.2 GPa experimentally⁵³ and 33.1 GPa theoretically⁴⁴) for this structure is in a good agreement with the value (28.5 GPa) calculated in our work. MoB_3 and MoB_4 were studied widely before^{43,44} and a few low-energy and in some cases hard structures were reported for these systems (i.e. $R\bar{3}m-MoB_3$ 31.8 GPa⁴³, $P6_3/mmc-MoB_3$ 37.3 GPa⁴⁴ and much softer $P6_3/mmc-MoB_4$ 8.2 GPa⁴⁴). In our work, however, new low-energy structures with high hardness were discovered for these systems (Table 1). For Mn_xB_y system, we propose a few new compounds in Table 1, which are simultaneously hard and low in energy. In a previous study⁵¹, $P2_1/c-MnB_4$ was discussed to be stable and have a very high hardness (40.1 GPa computationally⁵¹ and 34.6-37.4 GPa experimentally⁵²) and $C2/m-MnB_4$ was claimed to be the second low-energy structure with energy difference of 18 meV/atom. Our study confirms that the $P2_1/c-MnB_4$ is indeed the stable one. However, we discovered another MnB_4 structure with the space group $Pnmm$, with the energy intermediate between the energies of two previously proposed phases of MnB_4 (Table 1). In our work, it turned out that the ferromagnetic phase of $Pnmm-MnB_4$ is more stable than non-magnetic one, and the hardness of 40.7 GPa was computed for this magnetic structure. Because of the radioactivity of technetium, the Tc_xB_y system has not been studied experimentally (thus, there is no experimental result for comparison). However, computational studies on this system just started recently^{46,54-56}. In 2015, $P\bar{3}m1-TcB$ was predicted to be energetically more favorable than

previously discussed $Cmcm$ and WC-type structures⁵⁴. The reported hardness for this structure is 30.3 GPa⁵⁴, which is very close to the hardness of our predicted $P\bar{3}m1-TcB$ structure (31 GPa). It is worth mentioning that due to the discovery of other stable compounds (i.e. Tc_3B_5) in our work, this structure became slightly (13 meV/atom) above the convex hull. In our work, $P\bar{6}m2-TcB_3$ with predicted hardness 27.2 GPa, was discovered as a stable structure at zero pressure. However, in parallel to our work, this structure was also detected in other works^{55,56} and it was claimed that the structure is synthesizable under pressures above 4 GPa⁵⁵. In addition to this structure, we discovered another low-energy (3 meV above the convex hull) and hard structure (33.1 GPa) with $P\bar{3}m1$ space group for TcB_3 . $P\bar{6}m2-Tc_3B_5$ is another hard (30.6 GPa) and stable compound at zero pressure which is discovered in our work for the first time. Several other simultaneously hard (i.e. in the range of 30-36 GPa) and low-energy metastable phases of Tc_xB_y were discovered in our work and are shown in Table 1. During past years, many efforts have focused on searching for low-energy phases of V_xB_y and studying their electrical and mechanical properties. As a result, several low-energy hard and superhard phases were predicted^{48,49}. Nevertheless, the experimental data only exists for the well-known hexagonal $VB_2(AlB_2\text{-type})$ with $P6/mmm$ space group⁵⁰. In addition to some previously studied structures⁴⁹ (i.e. $Cmcm-VB$, $Immm-V_3B_4$ and $P6/mmm-VB_2$) which were also found in our calculations and are shown in Table 1 for comparison, a few boron-rich phases possessing simultaneously low energy and very high hardness were discovered (Table 1). The calculated hardness for these boron-rich phases is very close to or above 40 GPa (VB_7 : 39.7 GPa, VB_5 : 40 GPa and VB_{12} : 44.5 GPa). Extremely hard new $P\bar{4}m2-V_3B_4$ phase was discovered in our work, its energy is 6 meV lower than the previously proposed $Immm$

structure. Most of the studies on Fe_xB_y system were dedicated to FeB_2 and FeB_4 phases^{47,57,58}. Nevertheless, there are a few works studying different Fe_xB_y compounds^{60,61}. The reported stable phases are: Fe_2B , FeB and FeB_2 , but interestingly, in this work we detected another stable phase (FeB_3 with $P2_1/m$ space group and hardness 30.7 GPa), and to our knowledge FeB_3 was never reported, theoretically or experimentally. In the B_xP_y system, cubic boron phosphide BP with the zincblende structure is a well known compound; the hardness of this material was said to be roughly the same as of SiC ⁶². In our calculations, SiC was found to have hardness 33 GPa, while BP had 37 GPa. Moreover, B_6P was discovered as another stable compound in this system, and predicted to be superhard. The computed hardness of B_6P exceeds 41 GPa. For SiC system, in addition to the known β - SiC , with the diamond structure, another similar structure (actually, a polytype of β - SiC) with the space group $R3m$ and nearly the same hardness was found, the energy of this structure is 1 meV/atom higher than that of β - SiC . Mn_xH_y system is unexpected in the list of hard systems, but several very hard phases are indeed found (Table 1). All of these systems are non-magnetic, highly symmetric and energetically favorable (either on the convex hull or close to it), their hardness being up to 30 GPa. In this system, two thermodynamically stable compounds (Mn_2H and MnH) were discovered, with space groups $P\bar{3}m1$ and $P6_3/mmc$, and computed hardness of 21.5 GPa and 29.5 GPa, respectively (in Table 1, only structures with hardness value above 26 GPa are shown for this system). Generally, B_xS_y system is not hard, but metastable boron sulfides turn out to be potentially hard. We found a low-energy metastable phase of this system ($Cmcm$ - B_4S_3), the hardness of which unexpectedly exceeds 30 GPa. This can stimulate future studies of this system. For better insight, some of the prominent structures

seen in our simulations are shown in Fig 5a. More details on all phases from Table 1 are given in the Supplementary Information. In our calculation, some boron hydrides were predicted to be superhard, but these had high energy and not included in Table 1. However, it may be possible to stabilize these hard phases under pressure, or by chemical modification.

Fig 5b gives an Ashby plot "hardness - fracture toughness". Diamond and cubic BN possess the best properties, but are metastable at normal conditions; among stable phases, borides of transition metals (especially groups VB, VIB, VIIB) stand out: we note VB_2 , V_3B_4 , MoB_2 , CrB_4 , WB_5 and MnB_4 in particular. These and related materials possess high technological interest.

The fact that all known binary superhard systems were found in a short coevolutionary run demonstrates the power of our method, which is ready to be applied to other types of materials. For example, in addition to Mendeleevian search for stable/metastable hard and superhard materials, we performed another Mendeleevian search for stable/metastable magnetic materials to examine the power and efficiency of our method in fast and accurate determination of materials with target properties. In this calculation, well-known ferromagnets such as iron, cobalt, nickel and several magnetic materials (i.e. made from the combination of these elements with other promising elements) were detected within a few generations (before 6th generation). The chemical space in Mendeleevian searching for magnetic materials are shown in Fig 4(d-f) which was formed after calculating magnetization of 450 binary systems over 15 generations. It is clear from this figure that materials with high magnetization are clustered together. Fig 4d shows how the (co) evolutionary optimization discovered all the promising regions at the expense of unpromising regions (system

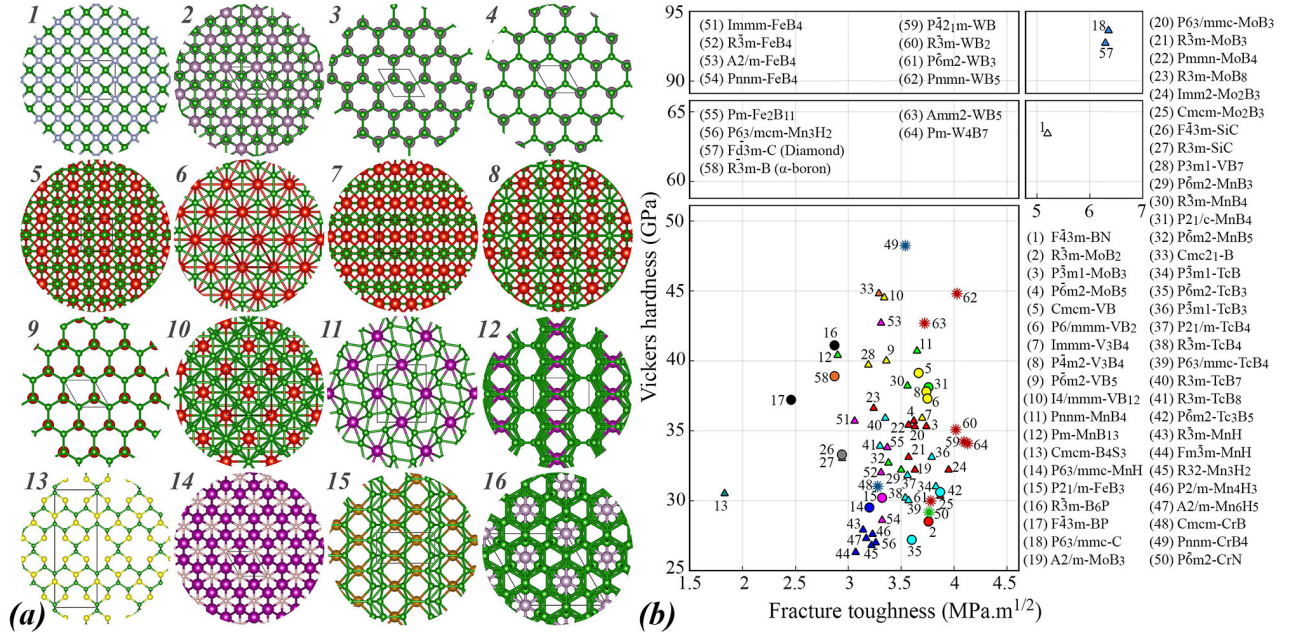


Figure 5: (a) (1) $F\bar{4}3m\text{-BN}$, (2) $R\bar{3}m\text{-MoB}_2$, (3) $P\bar{3}m1\text{-MoB}_3$, (4) $P\bar{6}m2\text{-MoB}_5$, (5) $Cmcm\text{-VB}$, (6) $P6/mmm\text{-VB}_2$, (7) $Immm\text{-V}_3B_4$, (8) $P\bar{4}m2\text{-V}_3B_4$, (9) $P\bar{6}m2\text{-VB}_5$, (10) $I4/mmm\text{-VB}_{12}$, (11) $Pnmm\text{-MnB}_4$, (12) $Pm\text{-MnB}_{13}$, (13) $Cmcm\text{-B}_4S_3$, (14) $P6_3/mmc\text{-MnH}$, (15) $P2_1/m\text{-FeB}_3$, (16) $R\bar{3}m\text{-B}_6P$. (b) Ashby plot⁶³ "hardness - fracture toughness". Suns are stable hard compounds from the previous works^{18,19}; circles represent stable compounds and triangles show metastable compounds in this work.

selection in the 5th and 10th generations are shown in Fig 4e and 4f).

5. Conclusion

We have developed a method for prediction of materials optimal in one or more target properties. The method is based on suitably defined chemical space, powerful evolutionary algorithm and multi-objective Pareto optimization technique. In this paper, we have examined our method by

Table 1: Predicted Vickers hardnesses (H_v), fracture toughness (K_{IC}) and enthalpies above the convex hull of selected materials found by MendS. Theoretical values from previous works are shown in parentheses and experimental values in brackets. Hardness was computed in this work using the Chen-Niu model¹⁶, and fracture toughness using the Niu-Niu-Oganov model¹⁷

	Compounds	H_v (GPa)	K_{IC} (MPa.m ^{1/2})	Instability (eV/atom)	Space group		Compounds	H_v (GPa)	K_{IC} (MPa.m ^{1/2})	Instability (eV/atom)	Space group
Carbon	<i>C</i>	92.7	6.33	0.13	$Fd\bar{3}m$	Boron	<i>B</i>	38.9	2.87	0	$R\bar{3}m$
	<i>C</i>	93.6	6.36	0.139	$P6_3/mmc$		<i>B</i>	44.8	3.29	0.136	$Cmc2_1$
B-S	B_4S_3	30.5	1.83	0.102	$Cmcm$	B-N	<i>BN</i>	63.4,(62.8)²⁵,[46-80]²⁰	5.1	0.075	$F\bar{4}3m$
Mo-B	MoB_2	28.5,(33.1) ⁴⁴ ,[24.2] ⁴³	3.76	0	$R\bar{3}m$	Tc-B	<i>TcB</i>	31,(30.3) ⁵⁴	3.83	0.013	$P\bar{3}m1$
	MoB_3	35.3	3.74	0.035	$P\bar{3}m1$		<i>TcB_3</i>	27.2,(29) ⁵⁵	3.6	0	$P\bar{6}m2$
	MoB_3	32.2	3.63	0.077	$A2/m$		<i>TcB_3</i>	33.1	3.79	0.003	$P\bar{3}m1$
		35.3,(37.3) ⁴⁴	3.63	0.017	$P6_3/mmc$		<i>TcB_4</i>	31.8	3.56	0.069	$P2_1/m$
		33.1,(31.8) ⁴³	3.57	0.011	$R\bar{3}m$		<i>TcB_4</i>	30.2	3.54	0.069	$R\bar{3}m$
	MoB_4	35.4	3.57	0.099	$Pnmm$			30,(32) ⁵⁵	3.57	0.027	$P6_3/mmc$
	MoB_5	35.7	3.62	0.054	$P\bar{6}m2$		<i>TcB_7</i>	35.9	3.35	0.084	$R3m$
	MoB_8	36.6	3.24	0.118	$R3m$		<i>TcB_8</i>	33.9	3.3	0.113	$R3m$
	Mo_2B_3	32.2	3.95	0.029	$Imn2$		Tc_3B_5	30.6	3.87	0	$P\bar{6}m2$
	Mo_2B_3	30.4	3.87	0.043	$Cmcm$						
Si-C	<i>SiC</i>	33.3,(33.1) ³¹ ,[28] ³¹	2.94	0	$F\bar{4}3m$	B-P	<i>BP</i>	37.2,(29.3) ³¹ ,[33] ³¹	2.46	0	$F\bar{4}3m$
	<i>SiC</i>	33.1	2.94	0.001	$R3m$		B_6P	41.1	2.87	0	$R\bar{3}m$
V-B	<i>VB</i>	39.1,(38.3) ⁴⁹	3.66	0	$Cmcm$	Mn-H	<i>MnH</i>	29.5	3.2	0	$P6_3/mmc$
	VB_2	37.3,(39.5) ⁴⁹ ,[27.2] ⁵⁰	3.75	0	$P6/mmm$		<i>MnH</i>	27.9	3.14	0.013	$R\bar{3}m$
	VB_5	40	3.36	0.158	$P\bar{6}m2$		<i>MnH</i>	26.3	3.07	0.044	$Fm\bar{3}m$
	VB_7	39.7	3.19	0.143	$P3m1$		Mn_3H_2	26.8	3.22	0.017	$R32$
	VB_{12}	44.5	3.34	0.125	$I4/mmm$		Mn_3H_2	27	3.26	0.019	$P6_3/mcm$
	V_3B_4	37.8	3.74	0	$P\bar{4}m2$		Mn_4H_3	27.6	3.23	0.002	$P2/m$
	V_3B_4	35.9,(38.2) ⁴⁹	3.7	0.006	$Immm$		Mn_6H_5	27.3	3.17	0.011	$A2/m$
Mn-B	MnB_3	32.2	3.5	0.029	$P\bar{6}m2$	Fe-B	FeB_3	30.2	3.32	0	$P2_1/m$
	MnB_4^\ddagger	40.7	3.65	0.009	$Pnmm$		FeB_4	35.7	3.06	0.021	$Immm$
	MnB_4	38.2	3.56	0.1	$R\bar{3}m$		FeB_4^\ddagger	32	3.31	0.039	$R\bar{3}m$
		38.1,(40.5) ³¹ ,[37.4] ⁵²	3.76	0	$P2_1/c$		FeB_4	42.7	3.31	0.063	$A2/m$
	MnB_5	32.7	3.38	0.097	$P\bar{6}m2$			28.6,(24.4) ⁶¹ ,[62] ⁵⁹	3.32	0.002	$Pnmm$
	MnB_{13}	40.4	2.9	0.181	Pm		Fe_2B_{11}	33.8	3.37	0.081	Pm

††For these phases we found that ferromagnetic solutions are more stable than non-magnetic. Elastic constant were computed assuming these are ferromagnetic structures, energy difference of magnetic and non-magnetic calculation for † and ‡ is 0.037 (eV/transition-metal) and 0.092 (eV/transition-metal) and magnetization is equal to 0.016 and 0.034 $\mu_B \cdot \text{\AA}^{-3}$, respectively.

searching for low-energy hard and superhard materials. Diamond, boron allotropes, and B-N system - famous superhard systems - were found in this single calculation together with other known hard systems (e.g, Si-C, B-C, Cr-N, W-C, metal borides, etc). Mn-H was discovered to be unexpectedly hard and several new hard and superhard phases were discovered in previously studied systems (i.e. V-B, Tc-B, Mn-B, etc). The method has successfully found almost all the known hard systems in this single run and a comprehensive chemical map of hard materials was produced. A similar chemical map was produced for magnetic materials; famous magnetic systems such as Ni, Co, Fe were found within a few generations. The examples of searches for hard materials and ferromagnets show the power and efficiency of the method. Using this method, one can search for materials optimal in any desired properties at arbitrary conditions, and this method is the first step in prediction of novel materials possessing desired properties, i.e. to a large extent it solves, in a fully non-empirical way, the central problem of computational materials science.

Acknowledgments We thank the Russian Science Foundation (grant 16-13-10459) and 5top100 project of MIPT for financial support. All the calculations were done using our supercomputer Rurik at Moscow Institute of Physics and Technology.

Author contributions A.R.O created the ideas behind the MendS method and the new Mendeleev numbers, Z.A. implemented the MendS algorithm and Pareto optimization, and performed all calculations, Z.A. and A.R.O wrote the paper.

References

1. S. Curtarolo et al., Predicting crystal structures with data mining of quantum calculations, *Phys. Rev. Lett.* 91 (2003) 135503.
2. R. Martoňák, A. Laio, M. Parrinello, Predicting crystal structures: The Parrinello-Rahman method revisited, *Phys. Rev. Lett.* 90 (2003) 075503.
3. A.R. Oganov, C.W.J. Glass, Crystal structure prediction using ab initio evolutionary techniques: Principles and applications, *Chem. Phys.* 124 (2006) 244704.
4. A.R. Oganov, H. Stokes, M. Valle, How evolutionary crystal structure prediction works; and why? *Acc. Chem. Res.* 44 (2011) 227-237.
5. A.O. Lyakhov, A.R. Oganov, et al., New developments in evolutionary structure prediction algorithm USPEX, *Comp. Phys. Comm.* 184 (2013) 1172-1182.
6. P. Villars, Sh. IWATA, Pauling file verifies/reveals 12 principles in materials science supporting four cornerstones given by Nature, *Chem. Met. Alloys.* 6 (2013) 81-108.
7. W.W. Zhang, A.R. Oganov, et al., Unexpected stoichiometries of stable sodium chlorides, *Science.* 342 (2013) 1502-1505.
8. Q. Zhu, A.R. Oganov, A.O. Lyakhov, Novel stable compounds in the Mg-O system under high pressure, *Phys. Chem. Chem. Phys.* 15 (2013) 7696-7700.
9. Q. Zhu, et al., Denser than diamond: ab initio search for superdense carbon allotropes, *Phys. Rev. B* 83 (2011) 193410.

10. D. G. Pettifor, A chemical scale for crystal-structure maps, *Solid State Commun.* 51 (1984) 31-34.
11. D. G. Pettifor, The structures of binary compounds. I. Phenomenological structure maps, *J. Phys. C: Solid State Phys.* 19(1986) 285-313.
12. Z. Allahyari, A.R. Oganov, Unpublished results.
13. A.R. Oganov, et al., Evolutionary crystal structure prediction as a method for the discovery of minerals and materials, *Rev. Mineral. Geochem* 71 (2010) 271-298.
14. M. Valle, A.R. Oganov, Crystal fingerprints space. A novel paradigm to study crystal structures sets, *Acta Cryst.* 66 (2010) 507–517.
15. A.O. Lyakhov, A.R. Oganov, Evolutionary search for superhard materials: Methodology and applications to forms of carbon and TiO₂, *Phys. Rev. B* 84 (2011) 092103.
16. X. Q. Chen, et al., Modeling hardness of polycrystalline materials and bulk metallic glasses, *Intermetallics* 19 (2011) 1275-1281.
17. H. Niu, et al., Simple and accurate model of fracture toughness of solids, arXiv:1805.05820v1 [cond-mat.mtrl-sci].
18. A.G. Kvashnin, et al., Computational search for novel hard chromium-based materials, *J. Phys. Chem. Lett.* 8 (4) (2017) 755–764.
19. A.G. Kvashnin, et al., New Tungsten Borides, Their Stability and Outstanding Mechanical Properties, *J. Phys. Chem. Lett.* 9 (12) (2018) 3470–3477.

20. V.V. Brazhkin, et al., Transformations of C_{60} fullerite under high-pressure high-temperature conditions, *Philos.Mag.A* 82 (2002) 231.
21. J. Haines, et al., Synthesis and design of superhard materials, *Annu. Rev. Mater. Res.* 31 (2001) 1.
22. T. Sasaki, et al., Simultaneous crystallization of diamond and cubic boron nitride from the graphite relative boron carbide nitride (BC_2N) under high pressure/high temperature conditions, *Chem.Mater.* 5 (1993) 695.
23. A.L. Liu, M.L. Cohen, Prediction of new low compressibility solids, *Science* 245 (1989) 841.
24. D.M. Teter, R.J. Hemley, Low-compressibility carbon nitrides, *Science* 271 (1996) 53.
25. Ch. He, et al., Z-BN: a novel superhard boron nitride phase, *Phys. Chem. Chem. Phys.* 14 (2012) 10967–10971.
26. Y. Li, et al., High-energy density and superhard nitrogen-rich B-N compounds, *Phys. Rev. Lett.* 115 (2015) 105502.
27. H. Hubert, et al., High-pressure, high-temperature synthesis and characterization of boron suboxide (B_6O), *Chem. Mater.* 10 (1998) 1530.
28. H.Y. Chung, et al., Synthesis of ultra-incompressible superhard rhenium diboride at ambient pressure, *Science* 316 (2007) 436.
29. A. Latini, et al., Superhard rhenium diboride films: preparation and characterization, *Chem. Mater.* 20 (2008) 4507.

30. Q. Gu, et al., Transition metal borides: superhard versus ultra-incompressible, *Adv. Mater.* 20 (2008) 3620.
31. F. Gao, Theoretical model of intrinsic hardness, *Phys. Rev. B* 73 (2006) 132104.
32. R. Riedel, Materials harder than diamond?, *Adv. Mater.* 4 (1992) 759.
33. F. Gao, et al., Hardness of covalent crystals, *Phys. Rev. Lett.* 91 (2003) 015502.
34. A. Simunek, J. Vackar, Hardness of covalent and ionic crystals: First-principle calculations, *Phys. Rev. Lett.* 96 (2006) 085501.
35. C.M. Sung, M. Sung, Carbon nitride and other speculative superhard materials, *Mater. Chem. Phys.* 43 (1996) 1.
36. J.M Leger, B. Blanzat, Materials potentially harder than diamond: Quenchable high-pressure phases of transition metal dioxides, *J. Mater. Sci. Lett.* 13 (1994) 1688.
37. J. Haines, J.M. Leger, Phase transitions in ruthenium dioxide up to 40 GPa: Mechanism for the rutile-to-fluorite phase transformation and a model for the high-pressure behavior of stishovite SiO_2 , *Phys. Rev. B* 48 (1993) 13344.
38. U. Lundin, et al., Transition-metal dioxides with a bulk modulus comparable to diamond, *Phys. Rev. B* 57 (1998) 4979.
39. J.V. Rau, A. Latini, New hard and superhard materials: $\text{RhB}_{1.1}$ and $\text{IrB}_{1.35}$, *Chem. Mater.* 21 (2009) 1407.

40. H.Y. Chung, et al., Correlation between hardness and elastic moduli of the ultraincompressible transition metal diborides RuB₂, OsB₂, and ReB₂, *Appl. Phys. Lett.* 92 (2008) 261904.
41. R.W. Cumberland, et al., Osmium diboride, an ultra-incompressible, hard material, *J. Am. Chem. Soc.* 127 (2005) 7264.
42. M. Hebbache, et al., A new superhard material: Osmium diboride OsB₂, *Solid State Commun.* 139 (2006) 227.
43. M. Zhang, et al., Structural modifications and mechanical properties of molybdenum borides from first principles, *J. Phys. Chem. C* 114 (2010) 6722–6725.
44. Y. Liang, et al., An unusual variation of stability and hardness in molybdenum borides, *Appl. Phys. Lett.* 101 (2012) 181908.
45. Ch. Xu, et al., A first-principles investigation of a new hard multi-layered MnB₂ structure, *RSC Adv.* 7 (2017) 10559.
46. H.J. Wu, G. Yang, Phase stability and physical properties of technetium borides: A first-principles study, *Comput. Mater. Sci.* 82 (2014) 86–91.
47. Y. Gou, et al., Electronic structures and mechanical properties of iron borides from first principles, *Solid State Commun.* 187 (2014) 28-32.
48. L. Wu, et al., Unraveling stable vanadium tetraboride and triboride by first-principles computations, *J. Phys. Chem. C* 119(37) (2015) 21649–21657.

49. Y. Pan, et al., Correlation between hardness and bond orientation of vanadium borides, RSC Adv. 4 (2014) 47377.
50. P. Wang, et al., Vanadium Diboride (VB_2) Synthesized at high pressure: Elastic, mechanical, electronic, and magnetic properties and thermal Stability, Inorg. Chem. 57(3) (2018) 1096–1105.
51. H. Nie, et al., Variable-composition structural optimization and experimental verification of MnB_3 and MnB_4 , Phys. Chem. Chem. Phys. 16 (2014) 15866.
52. H. Gou, et al., Peierls distortion, magnetism, and high hardness of manganese tetraboride, Phys. Rev. B. 89 (2014) 064108.
53. Sh. Okada, et al., Preparation of single crystals of MoB_2 by the aluminium-flux technique and some of their properties, J. Mater. Sci. 22 (1987) 2993-2999.
54. Zh. Gang-Tai, et al., New crystal structure and physical properties of TcB from first-principles calculations, Chin. Phys. B 24 (2015) 106104.
55. X. Miao, et al., Prediction on technetium triboride from first-principles calculations, Solid State Commun. 252 (2017) 40-45.
56. Ch. Ying, et al., New predicted ground state and high pressure phases of TcB_3 and TcB_4 : First-principles, Comput. Mater. Sci. 144 (2018) 154–160.
57. I. Harran, Exploring high-pressure FeB_2 : Structural and electronic properties predictions, J. Alloys Compd. 678 (2016) 109-112.

58. B. Li, et al., First-principles calculation of the indentation strength of FeB_4 , Phys. Rev. B 90 (2014) 014106.
59. H. Gou, et al., Discovery of a superhard iron tetraboride superconductor, Phys. Rev. Lett. 111 (2013) 157002.
60. A.N. Kolmogorov, et al., New superconducting and semiconducting Fe-B compounds predicted with an ab initio evolutionary search, Phys. Rev. Lett. 105 (2010) 217003.
61. L.H. Li, et al., First-principle calculations of structural, elastic and thermodynamic properties of Fe-B compounds, Intermetallics 46 (2014) 211-221.
62. K. Woo, K. Lee, K. Kovnir, BP: synthesis and properties of boron phosphide, Mater. Res. Express 3 (2016) 074003.
63. M.F. Ashby, Material property charts (chapter 4) of book: Materials Selection in Mechanical Design (4th Ed), Elsevier (2011) 57-96.